Journal of Neonatal Surgery
ISSN(Online): 2226-0439
Vol. 14, Issue 4s (2025)
https://www.jneonatalsurg.com

OPEN ACCESS

Canine Bone Repair and The Effects of Urinary Bladder Submucosa Implants

Hussein H. Nahi[*1], Duaa Raad Abd AlAmeer[2], Ahmed M. Amshawee[3], Maryam A. Hussain[4]

[*1]Surgery and obstrictic department, College of Veterinary Medicine, Al-Qasim Green University, Babylon 51013, Iraq. orcid.org/0000-0002-3474-1742.

[1]Al_taff university college Karbala, Iraq.

[2]College of Health and Medical Technology, AL-Zahraa University for Women Karbala, Iraq.

Email ID: duaa.r@alzahraa.edu.iq .orcid.org/0000-0001-7594-8283.

[3]Department of Radiology, University of Hilla, Babylon, Iraq.

Email ID: ahmed_meki@hilla-unc.edu.iq. orcid.org/0009-0007-5016-5697.

[4]Babylon Technical Institute, AL-Furat Al-Awsat Technical University, Babylon, Iraq.

Email ID: maryam.hussein.iba3@atu.edu.iq. orcid.org/0009-0001-8958-8079.

***Corresponding Author:**

Email ID: Husseinsur85@vet.uoqasim.edu.iq

Cite this paper as: Hussein H. Nahi, Duaa Raad Abd AlAmeer, Ahmed M. Amshawee, Maryam A. Hussain, (2025) Canine Bone Repair and The Effects of Urinary Bladder Submucosa Implants. *Journal of Neonatal Surgery*, 14 (4s), 1105-1117.

ABSTRACT

From the local strain, twenty adult male dogs were chosen. Two groups were formed from the dogs: the control group and the treatment group. To put the dogs to sleep, the anesthesiologists used a mix of xylazine and ketamine, with a dosage of 5 mg/kg of body weight for each. An electric drill was used to produce an 8 mm diameter hole in the distal part of the tibia in the control group. In the first week after surgery, the clinical results showed that edema, pain, and increased temperature at the operative site were more prominent in the treatment group compared to the control group, indicating inflammation. The treatment group reported a resolution of inflammatory symptoms four to five days after treatment, while the control group reported a resolution within six to seven days. According to the results of the radiographs, the sham response began in the first week of the trial for the treatment group but did not begin until the end of the third week for the control group. By the end of the third week of treatment, the control group no longer saw the line at all. By week four, the treatment group had witnessed the platelet bone re-establishing the bone bridge. When this happened, the contouring bones were restored because the outer callus merged with the bone. This study found that the healing of fractures was of higher quality and quantity in the treatment group compared to the control group. The treated group exhibited a significant increase in the growth and activity of osteoblasts, osteoclasts, and periosteal responses at the 15th and 30th days after the surgery. Additionally, there was a higher occurrence of osteocytes in the treated group compared to the control group

Keywords: *Canine bone repair, urinary bladder, submucosa*

1. INTRODUCTION

The incidence of orthopaedic fractures is significantly high, leading to substantial personal and societal costs and placing a heavy burden on hospital resources. The references used are Mackenzie et al., 1993 and Urquhart et al., 2006. Fractures are frequently observed in patients who have been hospitalised due to trauma. The reference is from Bradley and Harrison's work published in 2004. Explaining the epidemiology of orthopaedic injury in detail is challenging due to the diverse range of reported occurrences involving different types of fractures. Additionally, there are significant variations in geographical factors and methodological approaches that contribute to this complexity. Open fractures hold similar significance to closed fractures, despite the latter being more prevalent in terms of frequency. This is attributed to the intricacy of management, which frequently entails higher risks in terms of complications. Increased energy stress is also associated with open fractures, leading to more extensive damage to the soft tissues (MILLAR *ET AL.*, 2015)

Study has found that the annual occurrence of open long bone fractures is 11.5 per 100,000 individuals. The majority of these instances required hospitalisation and frequent complex surgeries, along with expensive rehabilitation requirements.

The citation is from MacKenzie et al., 2007. The prevalence of chronic pain often leads to impairment and work incapacity, in addition to the clinical consequences. The condition endured following the orthopaedic injury for a minimum of 12 months. (Urquhart et al., 2006There is a closing parenthesis. Significant emphasis has been placed on doing extensive study to explore the development of alternative natural and synthetic materials, as they are essential components for tissue transplants. The urinary bladder submucosa (UBS), obtained by separating the bladder tissue of warm-blooded vertebrates, was unexpectedly shown to possess comparable mechanical and biotropic characteristics to the submucosal layer of the intestine, as previously described in research. The study conducted by Badylak et al. in 1996 shown that it may serve as a viable substitute for intestinal submucosa tissue in a wide range of applications.

2. MATERIALS AND METHODS

Dogs:

Twenty mature mongrel dogs were selected from a group of strays. Over the duration of the trial, dogs weighing between fifteen and twenty kg were maintained in controlled environments to facilitate monitoring and acclimatization. After that, at the Veterinary Medicine faculty of Al-Qasim Green University, the dogs were put in pairs and kept in cages that were three by four metres long for the duration of the experiment.

Making the Matrix for the Urinary Bladder

The urinary bladders were sourced from cows that had been slaughtered not long before at the neighbourhood butcher. Then, according to the method outlined by Eberli et al. (2011), the UBM was built as a decellularized scaffold. What followed were the stages of this procedure:

The surplus collagenous connective and adipose tissues were eliminated from the exterior surfaces of the bladder using a pair of scissors. The complete excision of all layers of the urinary bladder, with the exception of the sub-mucosal layer, was achieved by reducing the intra-luminal water pressure, which caused the bladder to stretch and expand. (Fig. 3. 1). Next, the bladder was divided into a rectangular sheet form on one side, extending from its entrance to the apical area (Fig. 3.2).

- The mucosal layer was removed by incising the serosal layer-covered inferior bladder wall with a sharp knife edge. Similarly, the tunica serosa and tunica muscularis layers were removed by hand from the downward-positioned laminar side of the bladder. The final product looked like a bladder sheet: a flattened rectangle (Fig. 3.3). The tissue's submucosal layer was subsequently submerged in 7.4 pH phosphate buffered saline (PBS). The concentrations of penicillin, streptomycin, and ampicillin in the PBS solution were 100 IU/ml, 100 ug/ml, and 100 ug/ml, respectively. Representing the anatomy and physiology of the urinary bladder is the urine bladder matrix, or UBM.
- b. A mixture of 0.1% peracetic acid (PAA) and 4% ethanol was used to remove the non-collagen components of the UBM, which decreased the chances of host rejection. The next step was to let the mixture sit at room temperature for two hours while it was shaken. Careful planning and execution of the procedure ensured that the UBM's natural collagen structure and mechanical properties would remain intact. But the pH level was disturbed by the addition of peracetic acids all through the treatment. As a result, getting it back to a value of about 7.4 required totally removing all trace of par acetic acids. The technique was carried out as follows: A phosphate-buffered saline (PBS) solution was used to fully wash the extracellular matrix (ECM), which was then aggressively agitated. Following that, it was forcefully shaken and rinsed twice with water. The last step was to rinse it with PBS once again. The treatments were carried out at room temperature, with a 15-minute interval between each rinse. The resultant decellularized extracellular matrix (ECM) scaffolds were sterilised by soaking them for five hours at room temperature in a 0.1% peracetic acid (PAA) solution that had been pH-adjusted to 7.0 (Rosario et al., 2008).
- The scaffold, which had been decellularized and sterilised, was preserved at 4 °C in a sterile solution of PBS (phosphate buffer saline) that contained antibiotics and antifungal medications.

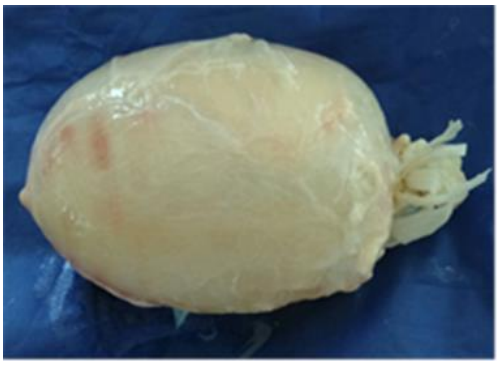

Figure 3.1: Bovine urinary bladder filled with water.

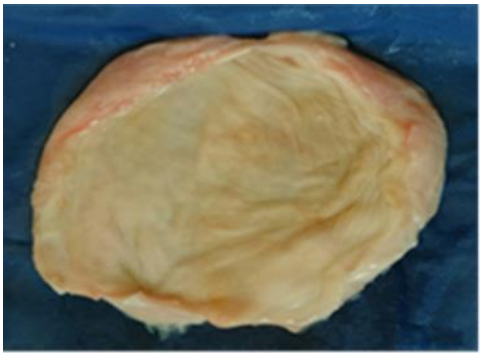

Figure 2: Opened urinary bladder wall.

Figure 3: Prepared sheet of bovine urinary bladder sub mucosa

Surgical procedure:

Before the surgery, the animals were fasted for 24 hours on food and 12 hours on water. The aseptic approach was used to disinfect the surgical site, which included the lower part of the tibia. The risk of postoperative infections was reduced by administering 10,000 units of penicillin and 20 mg/kg body weight of streptomycin intramuscularly one hour before to the surgery. Two intramuscular injections of atropine sulphate, 1 ml/kg of body weight, were given to the animals as a premedication. After fifteen minutes, an intramuscular injection of a mixture of three percent xylazine hydrochloride and five percent ketamine hydrochloride is given at a dose of twenty ml/kg of body weight. If needed, the dosage can be repeated half an amount at a time. While the animal was lying on its side, the operating region was encircled by surgical drapes (Fig. 1).

To create the 8 mm diameter hole in the tibia, a bit of drilling equipment was inserted into the middle of the bone. When this process is coupled with size 1 silk, a non-absorbable suture material, the outcomes are shown in Figure 2. To treat tunica vaginitis, absorbable suture material of 3/0 cat gut size is utilised. Lastly, the skin is sealed using a basic interrupted pattern of three or four silk thread stitches. To accomplish the same thing twice, you need to utilise a different cable. We used a 10% neutral buffered formalin solution to preserve the testicular samples after collection. Histopathological sections were made by following standard procedures; these sections were subsequently stained with Hematoxylin-Eosin and examined under a light microscope[6].

Experimental Design:

The dogs were randomly grouped into two (10 dog/group) as follow:

I. 1st group: Control group

Canines in this category, numbered 1–10, have a history of tibia fractures and have not had submucosal bladder treatments.

II. 2nd group: Treated group

The dogs in this group are assigned numbers 11-20 and have been diagnosed with tibia fractures. They have been treated using implanted urinary bladder submucosa.

Subsequently, the two groups were equally divided into subgroups for histopathology examination on the 15th and 30th day, respectively. They were also subjected to clinical, radiological, and histological testing.

Clinical examination

The dogs underwent a comprehensive examination, both physically and clinically, to assess their respiration rate, temperature, walking ability, heart rate, and presence of lameness. This evaluation took place within one week after the procedure.

Macroscopic evaluation:

Fracture sites in all animals are observed after 30 days following the procedure to examine the kind of fracture healing and the extent of callus development.

Radiological Examination:

Fracture healing was assessed weekly in both groups using a transportable X-ray machine (Kv 40, mAs 8) to conduct radiographic examinations. An photograph was captured of the animal in a side posture, showing a view of the tibia region from the side and middle. This was done 4 weeks after the procedure.

Histopathological findings:

Bone biopsies were conducted on the 15th and 30th day following the procedure. The biopsies were preserved in a solution of 10% buffered formalin, followed by treatment with alcohol and subsequent embedding in paraffin. Following the completion of the blocking process, the block was subjected to a staining technique using Hematoxylin and Eosin stain. This allowed for study of the block under a light microscope, with a focus on structures measuring 5-6 micrometres.

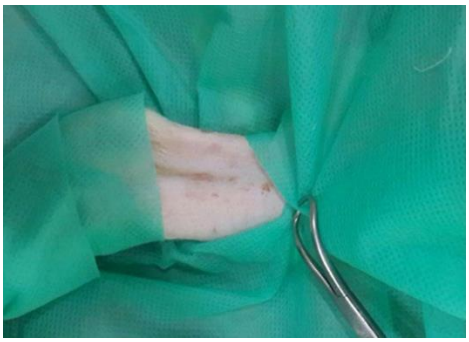

Figure 4: Photograph shows the site of operation.

Figure 5: The photograph depicts a hole in the tibia that was created in the distal portion of the bone using a drilling device.

Fig. 6: A photograph shows a borehole in the tibia, which was created in the lower part of the bone using a drilling equipment with a diameter of 8 mm.

3. RESULTS AND DISCUSSION

Clinical Examination:

The clinical examination identified many symptoms of inflammation, including swelling at the site of the surgery, increased temperature in the region, discomfort, and impaired capacity of the afflicted legs to bear weight, observed on the second day after the operation in the control group. The edoema diminished and the dogs regained the ability to support weight on the injured limb within a period of 5 to 6 days after the procedure.

However, the group that received treatment had distinct findings, with fewer indications observed. The indications subsequently diminished during a span of 4 days following the procedure. The presence of redness, swelling, heightened temperature at the surgical site, and discomfort observed on the second day after the surgery may be attributed to an augmentation in blood circulation to the operating region. In addition to that, it might be caused by the expansion of blood vessels and increased permeability of capillaries. As a result, it facilitated the movement of inflammatory cells, namely white blood cells, from the blood arteries to the site of operation, where edoema development occurred. The study was corroborated by Pharaon et al. (2018). The presence of edoema at the fracture site has exerted pressure on the nerve endings, resulting in discomfort. Inflammation severity increased prostaglandin synthesis, which stimulated vasodilation. As a consequence, there was a heightened infiltration of blood vessels with the accumulation of exudate at the site of the fracture. All of these indicators were diminished within a period of four to five days after the procedure in the control group. However, the treated group had a lower severity of clinical symptoms compared to the control group. The potential cause of this phenomenon might be attributed to the influence of thyroid hormones on blood vessels, which stimulates the generation of phagocytic cells at the surgical site. The presence of UBM caused an exacerbation of tissue inflammation by influencing the blood vessels through the introduction of authorised sources of different angiogenic and growth factors. The blood vessels grew into the adjacent tissue due to these factors, as supported by the findings of Matheny (2007) and Fiamingo et al. (2016). It was observed that the tearing of both the bone and surrounding tissue led to a deterioration in blood supply and an increase in acidity in the region. This tearing also caused a high exudation of white blood cells and plasma. These elements have resulted in the enlargement of the area and the necrotic tissues that were removed are experiencing severe inflammation.

Macroscopic evaluation:

Fracture sites in all animals are observed after 30 days post-operation to examine the kind of fracture healing and the extent of callus development.

1. Control group:

The macroscopic examination revealed a fracture that had repaired by secondary healing, characterised by a significant quantity of rough callus production with an uneven shape (Fig.7).

2. Treated group:

The macroscopic examination revealed that the bone fracture had undergone primary bone healing, with no presence of callus or just a minimal quantity of smooth callus growth (Fig.8).

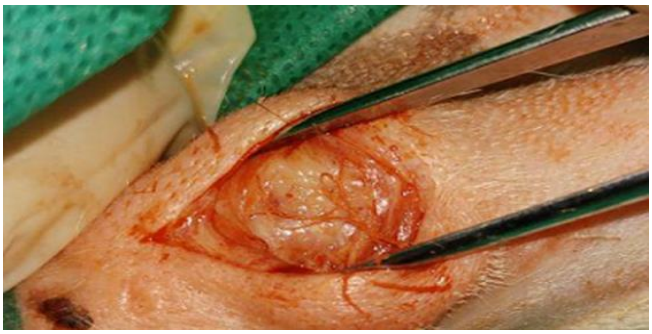

Figure 7: The macroscopic examination revealed the presence of secondary fracture healing and a significant quantity of rough callus development, which exhibited an uneven shape.

Figure 8: The macroscopic examination revealed primary bone healing with no evidence of callus or just a minimal degree of smooth callus development.

Radiological Findings:

The radiographic examination of the fracture site in both groups was conducted weekly to assess the extent of fracture healing. The outcomes were as follows: During the initial week following the procedure, both the control and treated groups had a distinct radiological sign characterised by a visible fracture site and soft tissue edoema, without any periosteal response. The control group did not show any noticeable alterations during the second week, while the treatment group displayed distinct fractures accompanied by the onset of periosteal response. During the first phase of the third week, the group that received treatment had periosteal reactivity that was located distant from the fracture line, as seen in Figure 4.

By the fourth week, the fracture in the treated group became imperceptible, and due to the subsequent remodelling, the bone has regained its original form.

1.Control Group:

1st week: There is no periosteral response surrounding the site, indicating a clean fracture (Fig. 4).

2nd week: There is no periosteal response surrounding the fracture, but the fracture itself is clearly visible (Fig.5).

3rd week: The fracture line is clearly apparent, accompanied by a little periosteal response that surrounds the fracture.

4th week: The periosteum reacts by forming a protective layer around the fracture. A callus is formed, which spans the gap and attempts to heal the hole, effectively creating a bridge. The fracture line is not visible (Fig.6).

2. **Treated Group**

1st week: The fracture does not show any periosteal response and the hole has clean margins with a clearly visible fracture (Fig.4).

2nd week: A mild periosteal response is observed at the location of the dramatic fracture (Fig.5).

3rd week: Periosteal reaction refers to the response of the periosteum, a layer of connective tissue that covers bones, to injury or inflammation. The callus forms throughout the whole location of the hole, bridging the gap and effectively filling it, making the fracture line undetectable.

4th week: An effort is made to unite the elongated bone and the creation of new bone with the bone's original shape, resulting in the bone potentially returning to its natural form (Fig. 6).

Fracture healing can occur in both callous and cortical bone, even in the absence of obvious callus formation. According to Wraighte and Scammell (2006), this kind of healing is known as primary bone healing when there is no production or replacement of apparent fracture callus The periosteum fails due to inadequate blood flow to the bone produced by reduced levels of thyroid hormones. This factor enhances the bone's metabolic rate by transporting osteogenic cells (Dallas et al., 2013; Bartl & Bartl, 2016).

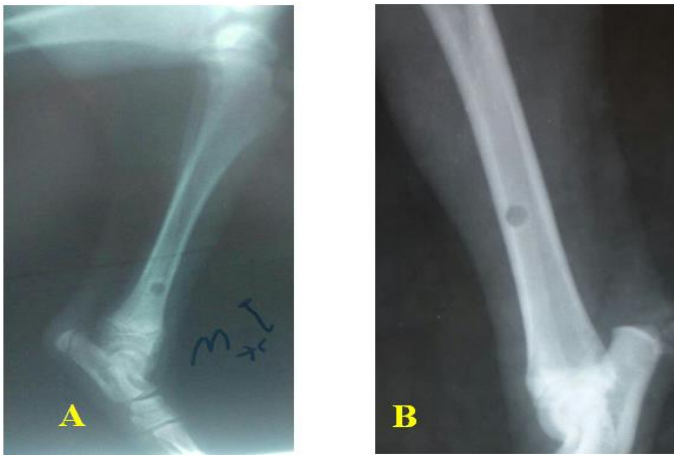

Figure 9: Initial radiographic imaging taken throughout the first week. A: Control group: The hole location does not exhibit any periosteral response and the fracture is clearly visible. B: In the treated group, there was no periosteal response observed at the fracture site. The fracture itself seemed clean, with smooth borders around the hole.

Fig. 10: Radiographic picture taken during the second week. A: Control group: No periosteal response observed surrounding the fracture, indicating a clean fracture. B: In the treated group, there was a mild periosteal response observed at the site of the hole, indicating a clear fracture.

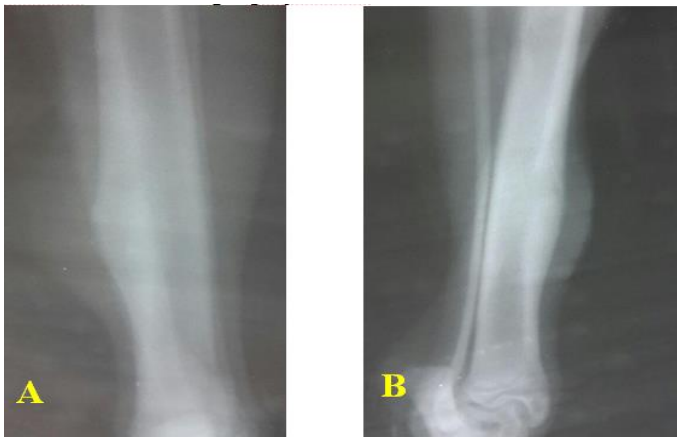

Fig. 11: 4th week radiographic picture. A: The control group attempts to create a bridge that fills the hole and makes the fracture line undetectable. Treatment group: There is a possibility of bone regrowth that matches the original bone shape, resulting in the bone returning to its native form.

4. HISTOLOGY

Control groups:

1. 1st subgroup on the 15th day post operation:

Histopathological analysis of the control group, conducted on the fifteenth post-operative day, showed the presence of connective tissue fibre bundles, inflammatory cells (including fibroblasts, macrophages, and neutrophils) (Fig.11). This resulted in fibrous tissue development and the presence of nuclei-free necrotic osteocytes in the lacunae. Figure 12.

2. 2nd subgroup on the 30th day post operation:

Histopathology results revealed a little degree of external callus development in the control group on day 30 following surgery. The metamorphosis of cartilage into bone tissue (Fig.13) provided evidence of this. Increased production of internal callus and proliferation of osteoclasts were brought about by the proliferation of osteoblasts, which lined the bone marrow. Compared to the 15th day, the regularity and thickness of the bone trabeculi increased throughout this period, while the size of the gaps between the trabeculi decreased. As shown in Figure 14.

Treated groups:

1. first subgroup on post-op day fifteen:

In the treated group, histopathology revealed the presence of clogged blood arteries and connective tissue fibres around the fracture site on the fifteenth day post-op. The structure was formed when fibroblasts invaded the fracture site and proliferated (Fig. 15).

The results showed that macrophages and plasma cells had infiltrated the area, along with connective tissue fibres. Bone trabeculae interspaces were narrowed. At this stage, osteoblast numbers skyrocketed, leading to the formation of osteoid tissue. When compared to the treated group, the control group showed a favourable correlation between increased thickness and regularity of bone trabeculi on day 15. The figures in question are Figures 16 and 17.

2. 2. On the 30th day after the procedure, second subgroup:

The histological analysis revealed an increase in the Haversian canal thickness and the formation of lamellar bone rather than compact bone throughout this time (Fig. 18). Bone trabeculae became thicker and more regularly arranged, and osteoblasts were shown to be proliferating. Increased bone plate thickness and homogeneity suggest the existence of internal callus (Fig. 19).

The following results were obtained from the histological examination of both groups:

At 15 days post-op, the cardinal symptoms were more noticeable in the control group than in the treatment group. This was because prostaglandin allowed fibroblasts and inflammatory cells (lymphocytes, monocytes, macrophages, and polymorphonuclear cells) to infiltrate. This triggers the formation of granulation tissue, migration of mesenchymal cells, and the subsequent expansion of vascular tissue. Calcification develops as a result of the breakdown of thyroid hormones, which initiates the process of delivering oxygen and nutrients to the exposed muscle and bone (Kalfas, 2001; Loi et al., 2016).

The treated group had more periosteal responses and proliferation of osteoblasts and osteoclasts at the 15th and 30th days after the operation, as compared to the control group. Furthermore, the control group exhibited a higher prevalence of osteocytes compared to the treated group. Possible explanations for this discrepancy include the administration of cytotoxic or anti-inflammatory medication in the initial week of treatment, which altered the inflammatory response and slowed down bone healing. Fibroblasts began depositing stroma during the healing phase, which paved the way for the formation of blood vessels. Present nicotine levels can impede capillary development (Boddupalli and Bratlie, 2016).

The formation of a collagen matrix and the secretion of mineralized osteoid occur in tandem throughout the progression of vascular ingrowth. A thin, flexible callus will form around the area of the injury. For the first four to six weeks after it heals, this callus does not have much mechanical strength. Internal fixation and bracing are necessary to provide adequate protection (Arazi and Canbora, 2016). Ossification of the callus joined the broken pieces of braided bone. But, if the immobilisation is not sufficient, the callus may not ossify, and an unstable fibrous union may develop (Noviana et al., 2011; Hyytiainen, 2016).

The vast presence of collagen in the body and its crucial role as a component of the extracellular matrix (ECM) have led many to consider it the most promising protein. Mild dispersion and hydrogen interactions, together with strong intermolecular cross-links, reinforce the collagen packing. Because collagen is insoluble in water, it provides the structural stability necessary for tissue formation (Halper & Kjaer, 2014; Wierer et al., 2018).

The elimination of bacteria caused the treated group to mature more rapidly during the remodelling stage. Everyone knew that this element needed oxygen to function. The chemotactic effects of UBM-derived growth factors, which boost neutrophil innate antibacterial activity, are responsible for the observed phenomena. Anaerobic organism suppression and

antibiotic (especially aminoglycoside) efficacy augmentation is another approach. To aid in wound healing, UBM growth factors promote fibroblast activity and the development of new blood vessels. Xing et al. (2016) and Kim et al. (2015) both state that these exercises will be a part of the management of soft tissue and orthopaedic injuries.

At this point in the healing process, the bone has returned to its original structure, mechanical strength, and shape; this is known as the remodelling stage of the fracture. As the bone remodels in response to mechanical stress, the healing process will be slow and steady, taking months or even years. Bone is usually deposited where it is needed and removed where it is not when the fracture site is subjected to an axial loading force, following the protocol outlined by (Kalfas, 2001; Mistry and Mikos, 2005; Liu *et al*., 2017; Eliaz and Metoki, 2017).

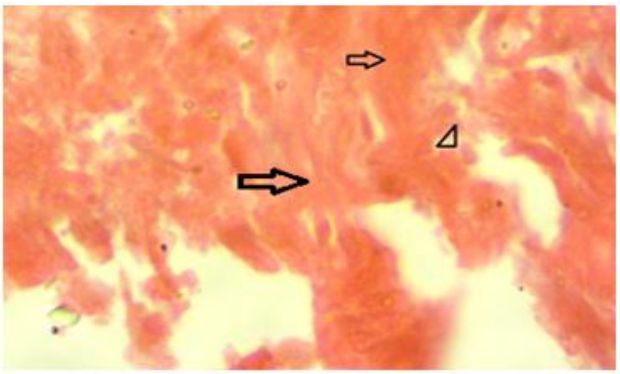

Figure (12) photomicrograph of control group at 15th day postoperation show presence of a network of fibrous tissue (⇨) and infiltration of inflammatory cells (◺)(H&E 100X).

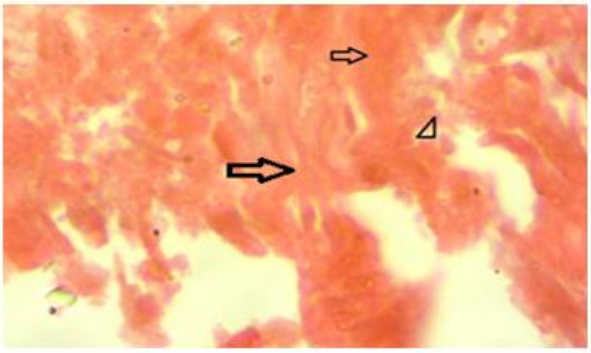

Figure (13) photomicrograph of control group at 15th day postoperation show fibrous tissue with presence the necrotic osteocyte that free of the nuclei in lacunae (H&E 100X).

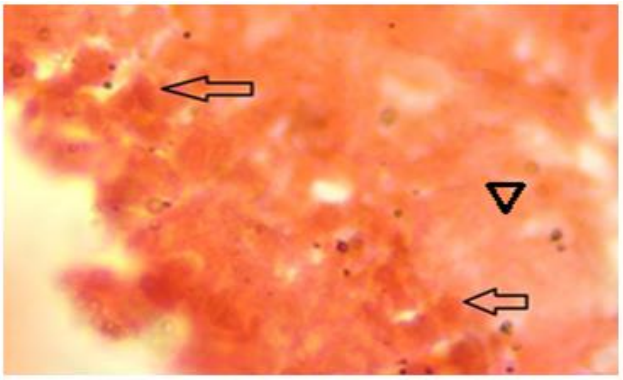

Figure (14) photomicrograph of control group at 30th day postoperation show external callus formation, that marked by the transformation of most of the cartilage tissue to bone tissue with prsence osteocyte (⇨)(H&E 100X).

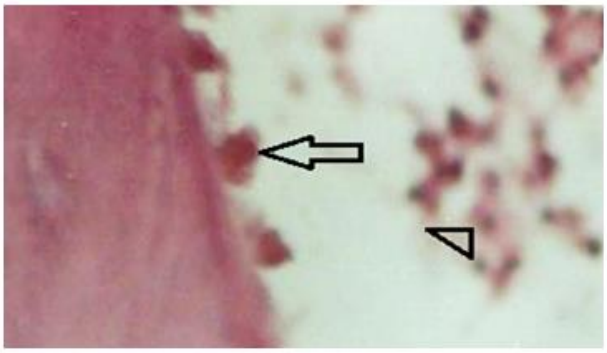

Figure (15) photomicrograph of control group at 30th day postoperation show proliferation of osteoblasts that lining the bone morrow and proliferation of osteoclast(◺)(H&E 100X).

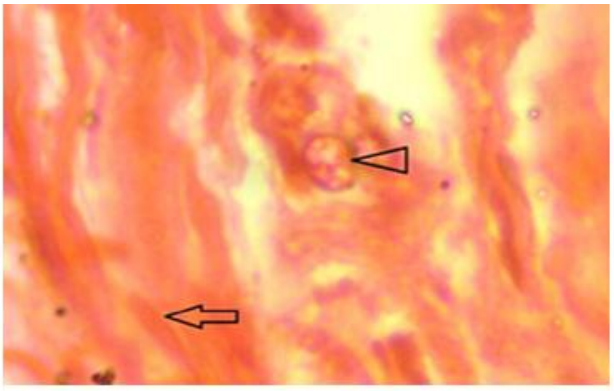

Figure (16) photomicrograph of treated group at 15th day postoperation show presence ofcongested blood vessels(⇒) around the fracture site with proliferation of fibroblast(◺)(H&E 100X).

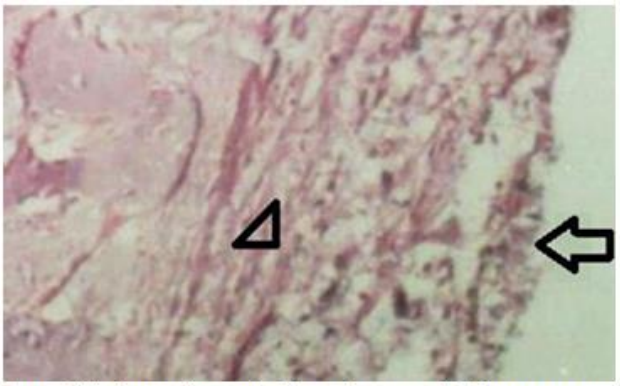

Figure (17) photomicrograph of treated group at 15th day postoperation show external callus formation that have little connective tissue fibers with infiltration with macrophages and plasma cells (H&E 40X).

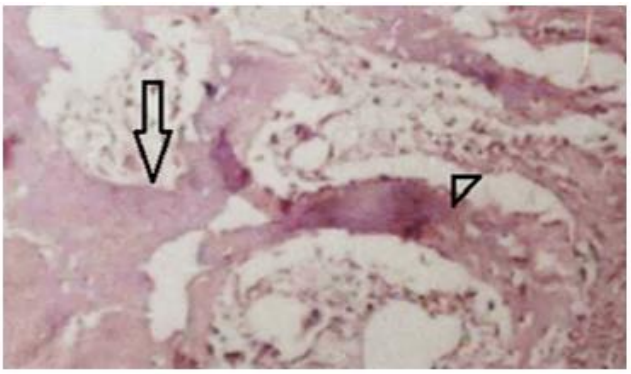

Figure (18) photomicrograph of treated group at 15th day postoperation show narrow gaps between bone trabeculi and proliferation of osteoblast that formed osteoid tissue (H&E 10X).

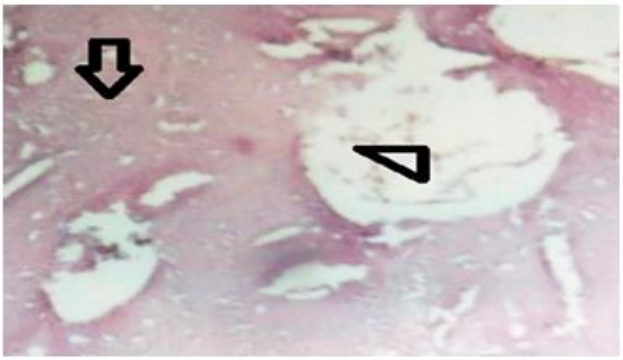

Figure (19) photomicrograph of treated group at 30th day postoperation show the lamellar bone formation instead of compact bone with increased in Haversian canal (H&E 10X).

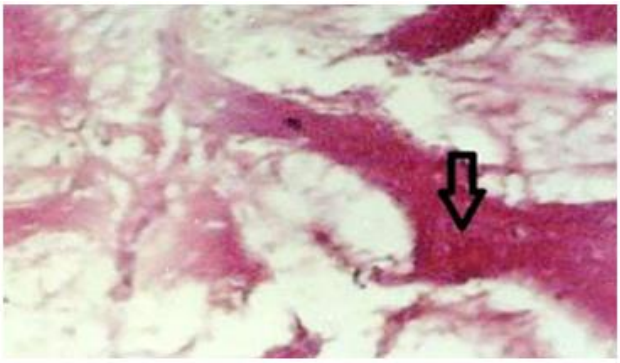

Figure (20) photomicrograph of treated group at 30th day postoperation show internal callus marked by more thickness and regularity of bone plate and increase in the thickness and regularity of bone trabeculi (⟹)(H&E 40X).

5. CONCLUSIONS

1. Inflammation was more severe in the placebo group than in the therapy group.

2. By the end of the second week, both the treated and control groups had shown signs of periosteal response, which means that the bone was beginning to repair at the fracture site.

4. At four weeks after surgery, the control group's fracture line was plainly visible, whereas the treated group did not.

5.Effects of the urinary bladder's submucosa on cells that repair damaged tissue In order to mend broken bones, collagen formation is essential.

REFERENCES

[1] MacKenzie EJ, Jones AS, Bosse MJ, et al. Health-care costs associated with amputation or reconstruction of a limb-threatening injury. J Bone Joint Surg Am 2007;89:1685–92.

[2] Urquhart DM, Edwards ER, Graves SE, et al. Characterisation of orthopaedic trauma admitted to adult Level 1 Trauma Centres. Injury 2006;37:120–7.

[3] Bradley C, Harrison J. Descriptive epidemiology of traumatic fractures in Australia. Injury research and statistics series. Adelaide: Australian Institute of Health and Welfare, 2004.

[4] Court-Brown CM, Rimmer S, Prakash U, et al. The epidemiology of open long bone fractures. Injury 1998;29:529–34 and Milar et al.,2015

[5] Millar, I. L., McGinnes, R. A., Williamson, O., Lind, F., Jansson, K. Å., Hajek, M. & Cameron, P. (2015). Hyperbaric Oxygen in Lower Limb Trauma (HOLLT); protocol for a randomised controlled trial. BMJ open, 5(6): 23-26.

[6] MacKenzie EJ, Jones AS, Bosse MJ. (2007). Health-care costs associated with amputation or reconstruction of a limb-threatening injury. J Bone Joint Surg Am. 89(12):1685–1692.

[7] Urquhart DM, Edwards ER, Graves SE. (2006). Characterisation of orthopaedic trauma admitted to adult Level 1 Trauma Centres. Injury. 37:120-127.

[8] Badylak, S. F., Voytik, S. L., Brightman, A., &Waninger, M. (2016). U.S. Patent No. 5,554,389. Washington, DC: U.S. Patent and Trademark Office. Matheny, R. G. (). U.S. Patent Application No. 14/452,707.

[9] Hodde, J. P., Badylak, S. F., and Shelbourne, K. D. (1997). The effect of range of motion on remodeling of small intestinal submucosa (SIS) when used as an Achilles tendon repair material in the rabbit. Tissue engineering. 3(1);27-37.

[10] Eberli, D.; Atala, A. and Yoo, J.J. (2011). One and four layer acellular bladder matrix for fascial tissue reconstruction. J. Mater Sci. Mater Med. 22:741-751.

[11] Pharaon, S. K., Schoch, S., Marchand, L., Mirza, A., and Mayberry, J. (2018). Orthopaedic traumatology: fundamental principles and current controversies for the acute care surgeon. Trauma Surgery & Acute Care Open. 3(1):110-117.

[12] Matheny, R. (2007). Compositions for reconstruction, replacement or repair of intracardiac tissue. U.S. Patent Application. 6(11):324,331.

[13] Fiamingo, A., Montembault, A., Boitard, S. E., Naemetalla, H., Agbulut, O., Delair, T., and David, L. (2016). Chitosan hydrogels for the regeneration of infarcted myocardium: preparation, physicochemical characterization, and biological evaluation. Biomacromolecules. 17(5): 1662-1672.

[14] Wraighte, P. J., &Scammell, B. E. (2006). Principles of fracture healing. Surgery-Oxford International Edition. 24(6): 198-207.

[15] Dallas, S. L., Prideaux, M., & Bonewald, L. F. (2013). The osteocyte: an endocrine cell and more. Endocrine reviews. 34(5): 658-690.

[16] Bartl, R., & Bartl, C. (2016). Bone Disorders: Biology, Diagnosis, Prevention, *Therapy. Springer.*11(3):113-119.

[17] Kalfas, I. H. (2001). Principles of bone healing. Neurosurgical focus, 10(4), 1-4.

[18] Loi, F., Cordova, L. A., Pajarinen, J., Lin, T. H., Yao, Z., and Goodman, S. B. (2016). Inflammation, fracture and bone repair Bone. 86:119-130.

[19] Boddupalli, A., Zhu, L., and Bratlie, K. M. (2016). Methods for Implant Acceptance and Wound Healing: Material Selection and Implant Location Modulate Macrophage and Fibroblast Phenotypes. Advanced healthcare materials. 5(20): 2575-2594.

[20] Noviana, D., Soedjono, G., Abdullah, D., Soehartono, R. H., Ulum, M. F., Siswandi, R., & Dahlan, K. A. (2011). In vivo study of hydroxyapatite-chitosan and hydroxyapatite-tricalcium phosphate bone graft in sheep's bone as animal model. In Instrumentation, Communications, Information Technology, and Biomedical Engineering (ICICI-BME), 2011 2nd International Conference on Pp. 403-408.

[21] Hyytiainen, H. (2016). Small animal treatment and rehabilitation for neurological conditions. Animal Physiotherapy: Assessment, Treatment and Rehabilitation of Animals. 23(5): 260.

[22] Halper, J., and Kjaer, M. (2014). Basic components of connective tissues and extracellular matrix: elastin, fibrillin, fibulins, fibrinogen, fibronectin, laminin, tenascins and thrombospondins. In Progress in Heritable Soft Connective Tissue Diseases (pp. 31-47). Springer, Dordrecht.

[23] Wierer, M., Prestel, M., Schiller, H. B., Yan, G., Schaab, C., Azghandi, S.&Aherrahrou, Z. (2018). Compartment-resolved Proteomic Analysis of Mouse Aorta during Atherosclerotic Plaque Formation Reveals Osteoclast-specific Protein Expression. Molecular & Cellular Proteomics. 17(2): 321-334.

[24] Kim, E. J., Choi, J. S., Kim, J. S., Choi, Y. C., & Cho, Y. W. (2015). Injectable and thermosensitive soluble extracellular matrix and methylcellulose hydrogels for stem cell delivery in skin wounds. Biomacromolecules. 17(1): 4-11.

[25] Xing, Q., Qian, Z., Jia, W., Ghosh, A., Tahtinen, M., & Zhao, F. (2016). Natural extracellular matrix for cellular and tissue biomanufacturing. ACS Biomaterials Science & Engineering. 3(8):1462-1476.

[26] Mistry, A. S., and Mikos, A. G. (2005). Tissue engineering strategies for bone regeneration. In Regenerative medicine II . Springer Berlin Heidelberg. Pp. 1-22.

[27] Liu, W. C., Chen, S., Zheng, L., and Qin, L. (2017). Angiogenesis Assays for the Evaluation of Angiogenic Properties of Orthopaedic Biomaterials–A General Review. Advanced Healthcare Materials. 12(3):123-128.

[28] Eliaz, N., and Metoki, N. (2017). Calcium Phosphate Bioceramics: A Review of Their History, Structure, Properties, Coating Technologies and Biomedical Applications. Materials. 10(4): 334.